

Conformational space annealing and an off-lattice frustrated model protein

Seung-Yeon Kim¹, Sung Jong Lee², and Jooyoung Lee^{1*}

¹School of Computational Sciences,

Korea Institute for Advanced Study,

207-43 Cheongryangri-dong, Dongdaemun-gu, Seoul 130-722, Korea

²Department of Physics and Center for Smart Bio-Materials,

The University of Suwon, Hwasung-si, Kyunggi-do 445-743, Korea

* correspondence to: jlee@kias.re.kr

Abstract

A global optimization method, conformational space annealing (CSA), is applied to study a 46-residue protein with the sequence $B_9N_3(LB)_4N_3B_9N_3(LB)_5L$, where B , L and N designate hydrophobic, hydrophilic, and neutral residues, respectively. The 46-residue BLN protein is folded into the native state of a four-stranded β -barrel. It has been a challenging problem to locate the global minimum of the 46-residue BLN protein since the system is highly frustrated and consequently its energy landscape is quite rugged. The CSA successfully located the global minimum of the 46-mer for all 100 independent runs. The CPU time for CSA is about seventy times less than that for simulated annealing (SA), and its success rate (100%) to find the global minimum is about eleven times higher. The amount of computational efforts used for CSA is also about ten times less than that of the best global optimization method yet applied to the 46-residue BLN protein, the quantum thermal annealing with renormalization. The 100 separate CSA runs produce the global minimum 100 times as well as other 5950 final conformations corresponding to a total of 2361 distinct local minima of the protein. Most of the final conformations have relatively small RMSD values from the global minimum, independent of their diverse energy values. Very close to the global minimum, there exist quasi-global-minima which are frequently obtained as one of the final answers from SA runs. We find that there exist two largest energy gaps between the quasi-global-minima and the other local minima. Once a SA run is trapped in one of these quasi-global-minima, it cannot be folded into the global minimum before crossing over the two large energy barriers, clearly demonstrating the reason for the poor success rate of SA.

I. INTRODUCTION

Finding the global minimum of a given function, called the global optimization, is an important problem in various fields of science and engineering. Many optimization problems are hard to solve since many of them belong to the NP-complete class, where the number of computing steps required to solve the problem increases faster than any power of the size of the system. Some of the well-known classic examples are the traveling salesman problem in applied mathematics and computer science, spin glasses in condensed-matter physics, and the protein-folding problem in biophysics.

Many of global optimization methods have been developed and successfully applied to a variety of problems. Examples of such methods are simulated annealing (SA)^{1,2}, genetic algorithm (GA)^{3,4}, Monte Carlo with minimization (MCM)⁵, multicanonical annealing^{6,7}, and quantum thermal annealing^{8,9,10}. One of the simplest algorithms for unbiased global optimization is the SA method which has been most widely used. Although the SA is very versatile in that it can be easily applied practically to any problem, the drawback is that its efficiency is usually much lower than problem specific algorithms. This is especially problematic for NP-complete problems. For this reason, it is important to find an algorithm which is as general as SA, and yet competitive with problem specific ones. Recently, a powerful global optimization method called conformational space annealing (CSA)^{11,12,13} was proposed, and applied to protein structure prediction^{14,15,16,17} and Lennard-Jones clusters¹⁸. The benchmark tests^{11,12,13} have demonstrated that it can not only find the known global-minimum conformations with less computations than existing algorithms, but also provide new global minima in some cases.

In this paper, we apply the CSA method to an off-lattice model protein introduced by Honeycutt and Thirumalai^{19,20,21}. The so-called BLN model proteins are constructed from the residues of three types, hydrophobic (B), hydrophilic (L), and neutral (N) residues found in nature. It is shown that they exhibit many similarities with real proteins. With the aid of simulation methods Honeycutt and Thirumalai studied a 46-residue BLN protein with the sequence $B_9N_3(LB)_4N_3B_9N_3(LB)_5L$ that folds into the native structure of a four-stranded β -barrel. They suggested the metastability hypothesis that a polypeptide chain may have a variety of metastable minima corresponding to folded conformations with similar structural characteristics but different energies. This hypothesis suggests that the particular state into

which a protein folds depends on the initial condition of the environment, and that there are multiple pathways for the folding process. Thirumalai *et al.*^{22,23} also demonstrated that the folding kinetics of the BLN 46-mer is very similar to that of real proteins. It is shown^{24,25,26,27} that the 46-mer has two characteristic transition temperatures: the transition from a random coil state to a collapsed but nonnative state and the transition from a collapsed state to the native β -barrel state. Subsequent studies^{28,29,30,31,32} illustrated that the 46-mer system exhibits a high degree of frustration and its energy landscape is very rugged. That is, there are many local minima with energies close to that of the native state, and it is very difficult to find the global minimum^{7,8,10,33}.

II. BLN MODEL PROTEIN

The potential energy of a BLN protein with M residues is given by

$$V = V_b + V_a + V_t + V_v, \quad (1)$$

where V_b is the bond-stretching energy, V_a the bond-angle bending energy, V_t the torsional dihedral-angle energy, and V_v the van der Waals energy. The bond-stretching energy is

$$V_b = \sum_{i=1}^{M-1} \frac{k_r}{2} (|\vec{r}_{i+1} - \vec{r}_i| - a)^2, \quad (2)$$

where the force constant is given by $k_r = 400\epsilon/a^2$, ϵ is the energy constant, a the average bond length, and \vec{r}_i the position of the i -th residue. The bond-angle bending energy is given by

$$V_a = \sum_{i=1}^{M-2} \frac{k_\theta}{2} (\theta_i - \theta_0)^2, \quad (3)$$

where the force constant is $k_\theta = 20\epsilon/(\text{rad})^2$, θ_i is the bond angle defined by three residues i , $i+1$ and $i+2$, and $\theta_0 = 1.8326$ rad or 105° . The torsional dihedral-angle energy is expressed as

$$V_t = \sum_{i=1}^{M-3} [A_i(1 + \cos \phi_i) + B_i(1 + \cos 3\phi_i)], \quad (4)$$

where ϕ_i is the dihedral angle defined by four residues i , $i+1$, $i+2$ and $i+3$. The amplitudes A_i and B_i are given by $A_i = 0$ and $B_i = 0.2\epsilon$ if two or more of the four residues are neutral. For all the other cases, $A_i = B_i = 1.2\epsilon$. Finally, the van der Waals energy is given by

$$V_v = 4\epsilon \sum_{i=1}^{M-3} \sum_{j=i+3}^M C_{ij} \left[\left(\frac{\sigma}{r_{ij}} \right)^{12} - D_{ij} \left(\frac{\sigma}{r_{ij}} \right)^6 \right], \quad (5)$$

where σ is the Lennard-Jones parameter and r_{ij} is the distance between non-bonded two residues i and j given by $r_{ij} = |\vec{r}_i - \vec{r}_j|$. If both residues i and j are hydrophobic, $C_{ij} = D_{ij} = 1$. If one residue is hydrophilic and the other hydrophilic or hydrophobic, $C_{ij} = 2/3$ and $D_{ij} = -1$. If one residue is neutral and the other neutral, hydrophilic or hydrophobic, $C_{ij} = 1$ and $D_{ij} = 0$. For convenience, we set $a = \epsilon = \sigma = 1$.

III. CONFORMATIONAL SPACE ANNEALING

The CSA unifies the essential ingredients of the three global optimization methods, SA, GA and MCM. First, as in MCM, we consider only the phase space of local minima, that is, all conformations are energy-minimized by a local minimizer. Secondly, as in GA, we consider many conformations (called a *bank* in CSA) collectively, and we perturb a subset of bank conformations (*seeds*) using the information in other bank conformations. This procedure is similar to mating in GA. However, in contrast to the mating procedure in GA, we replace typically *small* portions of a seed with the corresponding parts of bank conformations since we want to search the neighborhood of the seed conformation. Finally, as in SA, we introduce an annealing parameter D_{cut} (a cutoff distance in the phase space of local minima), which plays the role of temperature in SA. The diversity of sampling is directly controlled in CSA by introducing a distance measure between two conformations and comparing it with D_{cut} , whereas in SA there are no such systematic controls. The value of D_{cut} is slowly reduced just as in SA, hence the name *conformational space annealing*. Maintaining the diversity of the population using a distance measure was also tried in the context of GA, although no annealing was performed³⁴. To apply the CSA to an optimization problem, only two things are necessary; a method for perturbing a seed conformation, and a distance measure between two conformations. This suggests that the CSA is a candidate for a versatile and yet powerful global optimization method.

The way we picture the phase space of local minima is as follows (see Figure 1). We assume that most of the phase space of local minima can be covered by a finite number of large spheres with radius D_{cut} , which are centered on randomly chosen minima (*bank*). Each of the bank conformations is supposed to represent all local minima contained in the sphere centered on it. To improve a bank conformation A , we first select A as a seed. We perturb A and subsequently energy-minimize it to generate a trial conformation α . Since α originates

from A by small perturbation, it is likely that α is contained in a sphere centered on A . If the energy of α is lower than that of A , α replaces A and the center of the sphere moves from A to α . If it happens that α belongs to a different sphere centered on B , α can replace B in a similar manner. When α is outside of all existing spheres, a new sphere centered on α is generated. In this case, to keep the total number of spheres fixed, we remove the sphere represented by the highest-energy conformation. Obviously, the former two cases are more likely to happen when the spheres are large, and the latter when spheres are small. Consequently, larger value of D_{cut} produces more diverse sampling, whereas smaller value results in quicker search of low-energy conformations at the expense of getting trapped in a basin probably far away from the global minimum. Therefore, for efficient sampling of the phase space, it is necessary to maintain the diversity of sampling in the early stages and then gradually shift the emphasis toward obtaining low energy conformations, which is realized, in CSA, by slowly reducing the value of D_{cut} .

When the energy of a seed conformation does not improve after a fixed number of perturbations, we stop perturbing it. To validate this judgment, it is important that typical perturbations are kept small, so that the perturbed conformations are close to their original seeds. When all of the bank conformations are used as seeds (one iteration completed), this implies that the procedure of updating the bank might have reached a deadlock. If this happens we reset all bank conformations to be eligible for seeds again, and we repeat another iteration. After a preset number of iterations, we conclude that our procedure has reached a deadlock. When this happens, we enlarge the search space by adding more random conformations into the bank and repeat the whole procedure until the stopping criterion is met.

In the application of the CSA method to the BLN model protein (see Figure 2), we first randomly generate a certain number of initial conformations (for example, fifty random conformations) whose energies are subsequently minimized using Gay’s secant unconstrained minimization solver, SUMSL³⁵. In the following of the article the term *minimization* is used to refer to the application of SUMSL to a given conformation. We call the set of these conformations the *first bank*. We make a copy of the first bank and call it the *bank*. The conformations in the bank are updated in later stages, whereas those in the first bank are kept unchanged. Also, the number of conformations in the bank is kept unchanged when the bank is updated. The initial value of D_{cut} is set as $D_{\text{ave}}/2$ where D_{ave} is the average distance

between the conformations in the first bank. New conformations are generated by choosing a certain number of *seed* conformations (for example, ten seed conformations) from the bank and by replacing parts of the seeds by the corresponding parts of conformations randomly chosen from either the first bank or the bank. For example, five conformations are generated for each seed using the partial replacements. Then the energies of these conformations are subsequently minimized, and these minimized conformations become trial conformations.

A newly obtained local minimum conformation α is compared with those in the bank to decide how the bank should be updated. One first finds the conformation A in the bank which is closest to the trial conformation α with the distance $D(\alpha, A)$ defined by

$$D(\alpha, A) = \sum_{i=1}^{M-3} \min[\text{mod}(|\phi_i^\alpha - \phi_i^A|, 360^\circ), 360^\circ - \text{mod}(|\phi_i^\alpha - \phi_i^A|, 360^\circ)], \quad (6)$$

where $\text{mod}(A, B)$ is the least positive value of x satisfying $A = nB + x$ with an integer n . If $D(\alpha, A) < D_{\text{cut}}$, α is considered as similar to A . In this case, the conformation with lower energy among α and A is kept in the bank, and the other one is discarded. However, if $D(\alpha, A) > D_{\text{cut}}$, α is regarded as distinct from all conformations in the bank. In this case, the conformation with the highest energy among the bank conformations plus α is discarded, and the rest are kept in the bank. We perform this operation for all trial conformations.

After the bank is updated, the D_{cut} is reduced by a fixed ratio, in such a way that D_{cut} reaches $D_{\text{ave}}/5$ after L local minimizations (for example, $L = 500$). Then seeds are selected again from the bank conformations which have not been used as seeds yet, to repeat aforementioned procedure. The value of D_{cut} is kept constant after it reaches the final value. When all conformations in the bank are used as seeds, one round of iteration is completed. We perform an additional search by erasing the record of bank conformations having been used as seeds, and starting a new round of iteration. After three iterations are completed, we increase the number of bank conformations by adding fifty randomly generated and minimized conformations into the bank (and also into the first bank), and reset D_{cut} to $D_{\text{ave}}/2$. The algorithm stops when the known global minimum is found, which is examined after the bank is updated by all trial conformations. It should be noted that since one iteration is completed only after all bank conformations have been used as seeds, and we add random conformations whenever our search has reached a deadlock, there is no loss of generality for using particular values for the number of seeds, the number of bank

conformations, etc.

IV. RESULTS AND DISCUSSION

We applied the CSA method to the BLN 46-mer with the sequence $B_9N_3(LB)_4N_3B_9N_3(LB)_5L$. We carried out 100 independent runs and found the global minimum-energy conformation with energy

$$E_0 = -49.2635 \tag{7}$$

for all 100 runs. Figure 3 shows a scatter plot of the number of function evaluations to obtain the global minimum-energy conformation for 100 independent runs. On average, it took about 1.865×10^6 function evaluations for each run. The total running time for all 100 runs was 48 hours and 8 minutes on an Athlon processor (1.8 GHz). For a single run it took only about 29 minutes on average to obtain the global minimum-energy conformation. For the 46-mer, it is reported^{8,10} that the average success rate to reach the global minimum is about 9% using SA with 32×10^6 Monte Carlo sweeps (1 Monte Carlo sweep = 46 Monte Carlo steps). For the purpose of fair benchmarking, we also carried out hundreds of the SA runs and we found that our results are consistent with these numbers. A single run of SA with 32×10^6 Monte Carlo sweeps took about 34 hours on the same Athlon processor. Therefore, the CPU time for CSA is about seventy times less than that for SA, and its success rate (100%) is about eleven times higher. Until now, the best method to obtain the global minimum of the 46-mer has been the quantum thermal annealing with renormalization (QTAR)¹⁰. The QTAR method has been the only method with 100% success rate and yet requires 7.5 times less computation than SA. Therefore, compared to QTAR, CSA is about ten times more efficient in finding the global minimum of the BLN 46-mer.

One of the attractive aspects of CSA is that a population of distinct local minima is obtained as a by-product, in addition to the global minimum-energy conformation. Gathering all conformations in the final banks of 100 independent CSA runs, we have obtained a total of 6050 conformations all together. The conformation with the highest energy among the 6050 conformations has the energy

$$E_h = -36.355. \tag{8}$$

Table I shows the energy spectrum of these 6050 conformations. There are 2361 different energy levels between E_0 and E_n . As the energy level becomes higher, the number of energy levels increases fast. This implies that conformations near the global minimum are discretely distributed but conformations at higher energies are quasi-continuum states. In Table I the number of energy levels decreases for $E > -43$ due to the fact that conformations of high energies are discarded as a CSA run proceeds. Figure 4 shows the number of conformations as a function of energy for $E \leq -48$. It should be noted that there exist two largest energy gaps

$$\Delta E_a = 0.201 \tag{9}$$

between $E_5 = -48.939$ and $E_6 = -48.738$ and

$$\Delta E_b = 0.138 \tag{10}$$

between $E_8 = -48.731$ and $E_9 = -48.593$.

Since the potential energy of BLN model proteins is invariant under the inversion transformation

$$\vec{r}_i \rightarrow -\vec{r}_i \quad \text{or} \quad \phi_i \rightarrow -\phi_i, \tag{11}$$

two conformational states exist for each energy level (two-fold degeneracy), including the global minimum-energy conformation. The root-mean-square deviation (RMSD) between the two global minima is 0.862. The inversion symmetry is employed in CSA by generating conformations with positive values only for the first dihedral angle ϕ_1 ($0 \leq \phi_1 \leq 180$). Figure 5 shows the RMSD values as a function of energy for all 2361 conformations with $0 \leq \phi_1 \leq 180$, calculated from the global minimum. In Figure 5 most of the 2361 conformations have small values of RMSD from the global minimum, independent of their diverse energy values. These conformations are grouped together in the region $\text{RMSD} < 1.6$, separated from conformations with larger values of RMSD. The number of conformations with RMSD values less than 1.6 is 2215, which is 93.8% of all conformations. It is quite interesting to observe that no conformations with energy less than -44.34 appear in the region $\text{RMSD} > 1.6$. We also performed 100 CSA runs without employing the inversion symmetry. The results are quite similar to those in Table I and Figures 3, 4, and 5, and finding the global minimum requires about 1.4 times more computation.

Now we examine the RMSD-versus-energy distribution for conformations near the global-minimum energy E_0 in detail. Figure 6 is an enlargement of the lower left corner of Figure

5 for $E \leq -48$. Similarly, Figure 7 shows the results with $-180 \leq \phi_1 \leq 180$. The values of RMSD are calculated from one of the two global minima. The RMSD distribution calculated from the other global minimum is similar to Figure 7. The twelve (six pairs) conformations below the largest gap ΔE_a (Eq. (9)) in Figure 7 are of two branches, which are related to each other by the inversion transformation. We call ten of these conformations ($E_1 = -49.186$, $E_2 = -49.149$, $E_3 = -49.063$, $E_4 = -49.002$, and $E_5 = -48.939$) as quasi-global-minima, since they are more frequently obtained as final candidates for global minimum, in SA, than the native state is. Once a SA run is trapped into one of these quasi-global-minima, the trapped conformation cannot be folded into the global minimum before crossing over the two large energy barriers of Eqs. (9) and (10). This clearly demonstrates the reason for the poor success rate of SA. On the other hand, the RMSD values for the conformations above the energy gap are scattered between 0.15 and 1.2. In particular, conformations with energy $E_8 = -48.731$ (RMSD = 0.156, 0.881) can be easily folded into the native state without being trapped in one of the quasi-global-minima.

V. CONCLUSION

We have applied the versatile and powerful global optimization method, conformational space annealing, to the 46-residue BLN protein with a sequence $B_9N_3(LB)_4N_3B_9N_3(LB)_5L$. The CSA method always maintains the diversity of sampling and is able to cross the high energy barriers between local minima. Consequently, this method not only finds the global minimum-energy conformation successfully and efficiently but also investigates many other distinct local minima as a by-product.

This 46-residue BLN protein is folded into the native state of a four-stranded β -barrel. It has been a challenging problem to locate the global minimum of the BLN 46-mer because the molecule is highly frustrated and its energy landscape is quite rugged. We conducted 100 independent CSA runs and successfully found the global minimum-energy conformation of the 46-residue BLN protein for all 100 runs. The CPU time for CSA is about seventy times less than that for simulated annealing, and its success rate (100%) to find the global minimum is about eleven times higher. In addition, the amount of computational efforts required for CSA to find the global minimum is about ten times less than that for the QTAR, the best global optimization method yet applied for the 46-residue BLN protein.

The 100 separate CSA runs produce the global minimum 100 times as well as other 5950 final conformations corresponding to 2360 distinct local minima of the 46-residue BLN protein. As the values of energy levels becomes higher, the number of energy levels (or the number of local minima) increases fast. Conformations near the global minimum are discretely distributed but conformations of higher energies are quasi-continuum states. Most of final conformations have relatively small RMSD values from the global minimum, independent of their diverse energy values. Very close to the global minimum, there exist quasi-global-minima which are frequently obtained as one of the final answers from SA runs. We find that there exist two largest energy gaps between the quasi-global-minima and the other local minima. Once a SA run is trapped in one of these quasi-global-minima, it cannot be folded into the global minimum before crossing over the two large energy barriers, clearly demonstrating the reason for the poor success rate of SA.

Acknowledgments

We are grateful to Prof. Julian Lee for useful discussions and for kindly drawing Figure 1.

-
- ¹ S. Kirkpatrick, C. D. Gelatt, and M. P. Vecchi, *Science* **220**, 671 (1983).
- ² P. van Laarhoven and E. H. L. Aarts, *Simulated Annealing: Theory and Applications* (Kluwer, Dordrecht, 1992).
- ³ J. Holland, *SIAM J. Comput.* **2**, 88 (1973).
- ⁴ D. E. Goldberg, *Genetic Algorithms in Search, Optimization, and Machine Learning* (Addison Wesley, Reading, MA, 1989).
- ⁵ Z. Li and H. A. Scheraga, *Proc. Natl. Acad. Sci. USA* **84**, 6611 (1987).
- ⁶ J. Lee and M. Choi, *Phys. Rev. E* **50**, 651 (1994).
- ⁷ H. Xu and B. J. Berne, *J. Chem. Phys.* **112**, 2701 (2000).
- ⁸ Y.-H. Lee and B. J. Berne, *J. Phys. Chem. A* **104**, 86 (2000).
- ⁹ Y.-H. Lee and B. J. Berne, *Ann. Phys. (Leipzig)* **9**, 668 (2000).
- ¹⁰ Y.-H. Lee and B. J. Berne, *J. Phys. Chem. A* **105**, 459 (2001).
- ¹¹ J. Lee, H. A. Scheraga, and S. Rackovsky, *J. Comput. Chem.* **18**, 1222 (1997).
- ¹² J. Lee, H. A. Scheraga, and S. Rackovsky, *Biopolymers* **46**, 103 (1998).
- ¹³ J. Lee and H. A. Scheraga, *Int. J. Quantum Chem.* **75**, 255 (1999).
- ¹⁴ J. Lee, A. Liwo, and H. A. Scheraga, *Proc. Natl. Acad. Sci. USA* **96**, 2025 (1999).
- ¹⁵ A. Liwo, J. Lee, D. R. Ripoll, J. Pillardy, and H. A. Scheraga, *Proc. Natl. Acad. Sci. USA* **96**, 5482 (1999).
- ¹⁶ J. Lee, A. Liwo, D. R. Ripoll, J. Pillardy, and H. A. Scheraga, *Proteins* **S3**, 204 (1999).
- ¹⁷ J. Lee, A. Liwo, D. R. Ripoll, J. Pillardy, J. A. Saunders, K. D. Gibson, and H. A. Scheraga, *Int. J. Quantum Chem.* **77**, 90 (2000).
- ¹⁸ J. Lee, I.-H. Lee, and J. Lee, Unbiased global optimization of Lennard-Jones clusters for $N \leq 201$ by conformational space annealing method, submitted to *Phys. Rev. Lett.*
- ¹⁹ J. D. Honeycutt and D. Thirumalai, *Proc. Natl. Acad. Sci. USA* **87**, 3526 (1990).
- ²⁰ J. D. Honeycutt and D. Thirumalai, *Biopolymers* **32**, 695 (1992).
- ²¹ T. Veitshans, D. Klimov, and D. Thirumalai, *Folding Des.* **2**, 1 (1997).
- ²² Z. Guo, D. Thirumalai, and J. D. Honeycutt, *J. Chem. Phys.* **97**, 525 (1992).
- ²³ D. Thirumalai and Z. Guo, *Biopolymers* **35**, 137 (1995).
- ²⁴ Z. Guo and D. Thirumalai, *Biopolymers* **36**, 83 (1995).

- ²⁵ Z. Guo and C. L. Brooks, *Biopolymers* **42**, 745 (1997).
- ²⁶ Z. Guo and D. Thirumalai, *Folding Des.* **2**, 377 (1997).
- ²⁷ J.-E. Shea, Y. D. Nochomovitz, Z. Guo, and C. L. Brooks, *J. Chem. Phys.* **109**, 2895 (1998).
- ²⁸ R. S. Berry, N. Elmaci, J. P. Rose, and B. Vekhter, *Proc. Natl. Acad. Sci. USA* **94**, 9520 (1997).
- ²⁹ H. Nymeyer, A. E. Garcia, and J. N. Onuchic, *Proc. Natl. Acad. Sci. USA* **95**, 5921 (1998).
- ³⁰ N. Elmaci and R. S. Berry, *J. Chem. Phys.* **110**, 10606 (1999).
- ³¹ M. A. Miller and D. J. Wales, *J. Chem. Phys.* **111**, 6610 (1999).
- ³² D. A. Evans and D. J. Wales, *J. Chem. Phys.* **118**, 3891 (2003).
- ³³ P. Amara and J. E. Straub, *J. Phys. Chem.* **99**, 14840 (1995).
- ³⁴ B. Hartke, *J. Comput. Chem.* **20**, 1752 (1999).
- ³⁵ D. M. Gay, *ACM Trans. Math. Software* **9**, 503 (1983).

TABLE I: The energy spectrum of 6050 final conformations for all 100 independent runs of CSA. NE is the number of energy levels for a given energy range, NC is the number of conformations for a given energy range, and DC is the density of conformations (the number of conformations per energy level, that is, $DC = NC/NE$). The total number of energy levels is 2361.

energy range	NE	NC	DC
$E_0 \leq E \leq -49$	5	295	59.00
$-49 < E \leq -48$	31	722	23.29
$-48 < E \leq -47$	111	1033	9.31
$-47 < E \leq -46$	192	699	3.64
$-46 < E \leq -45$	297	689	2.32
$-45 < E \leq -44$	374	766	2.05
$-44 < E \leq -43$	377	624	1.66
$-43 < E \leq -42$	353	517	1.46
$-42 < E \leq -41$	263	319	1.21
$-41 < E \leq -40$	159	181	1.14
$-40 < E \leq -39$	110	114	1.04
$-39 < E \leq -38$	50	51	1.02
$-38 < E \leq -37$	27	28	1.04
$-37 < E \leq E_h$	12	12	1.00

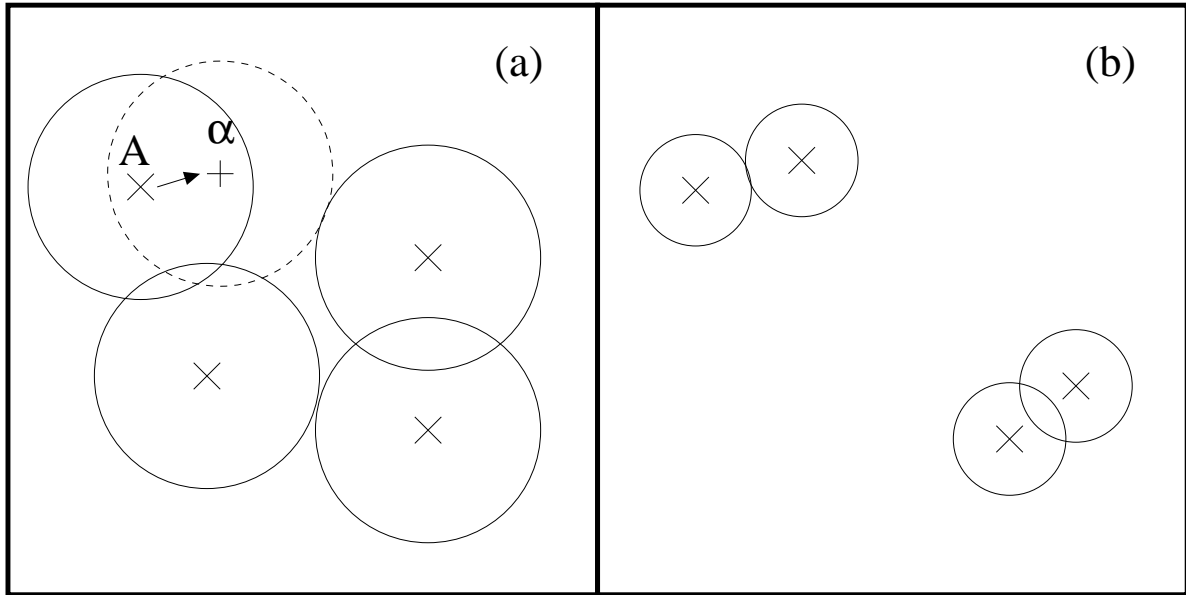


FIG. 1: A schematic for the search procedure of CSA. The boxes represent the identical phase space. (a) Initially, we cover the phase space by large spheres centered on randomly chosen local minima denoted by \times symbols, and replace the centers with lower-energy local minima. When an initial conformation A is replaced by a new conformation α , the sphere moves in the direction of the arrow. (b) As the CSA algorithm proceeds and the energies of the representative conformations at the centers of the spheres are lowered, the size of the spheres are reduced and the search space is narrowed down to small basins of low-lying local minima.

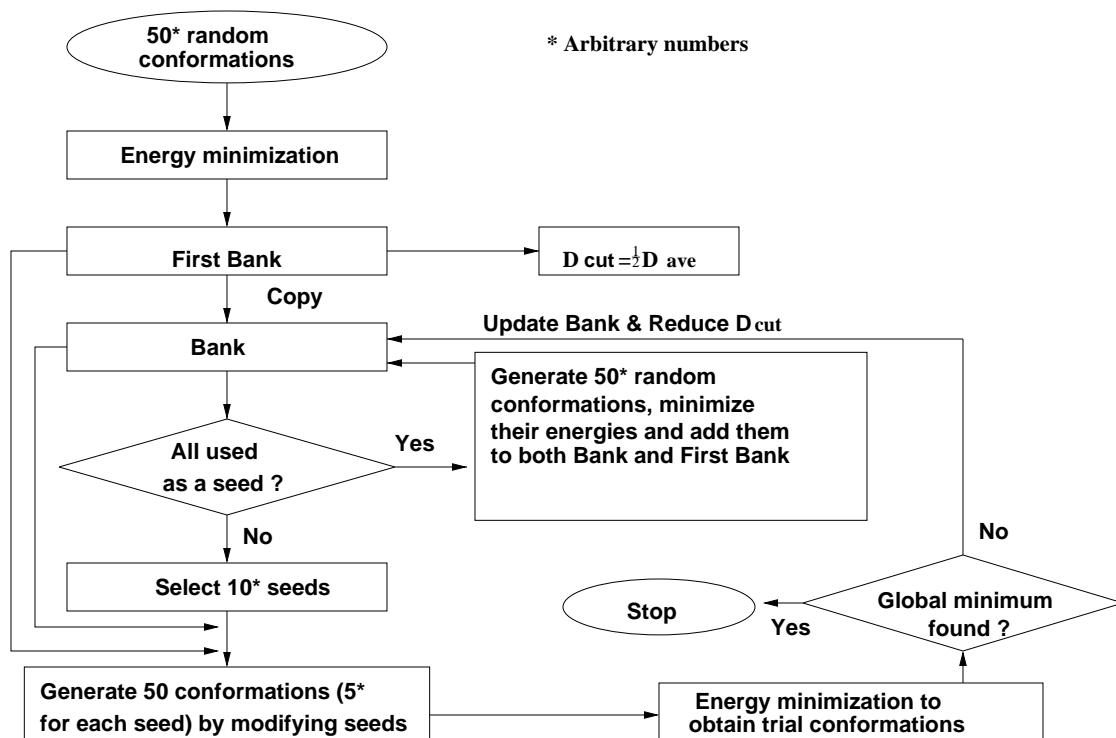


FIG. 2: Flow chart of the CSA algorithm to locate the global minimum of a BLN model protein.

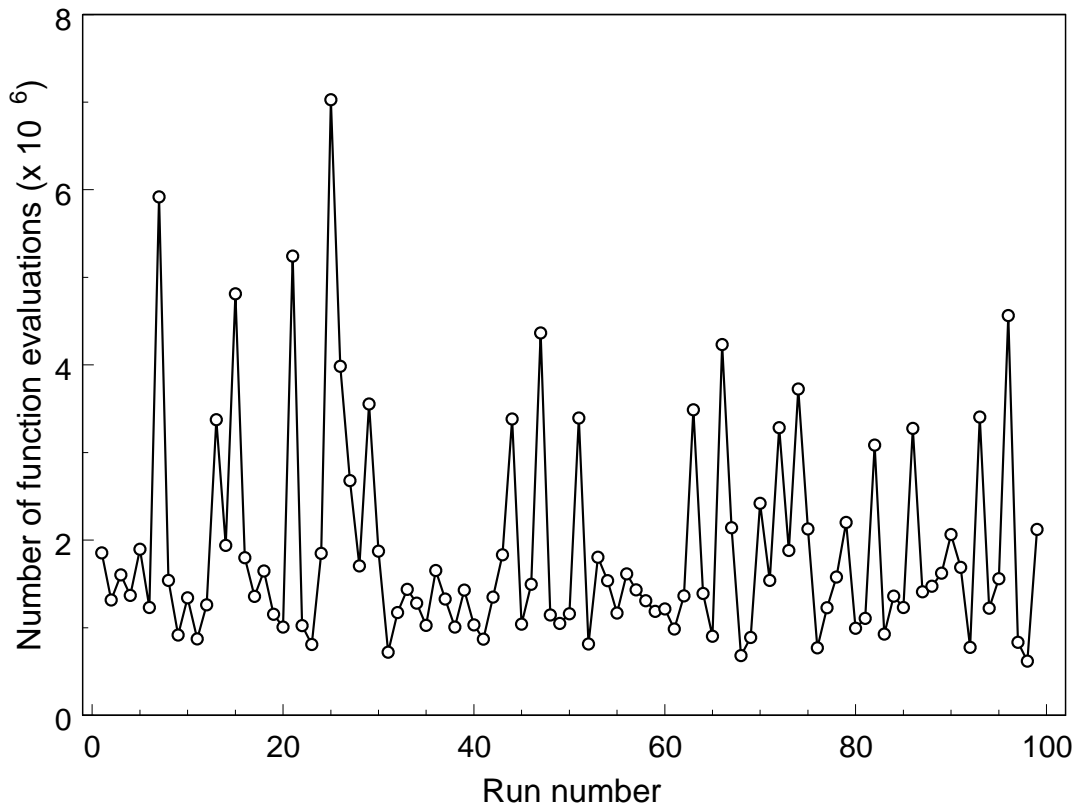


FIG. 3: Scatter plot of the number of function evaluations to obtain the global minimum-energy conformation with energy $E_0 = -49.2635$ for 100 independent runs. The global minimum-energy conformation was successfully obtained for all 100 independent runs with about 1.865×10^6 function evaluations on average.

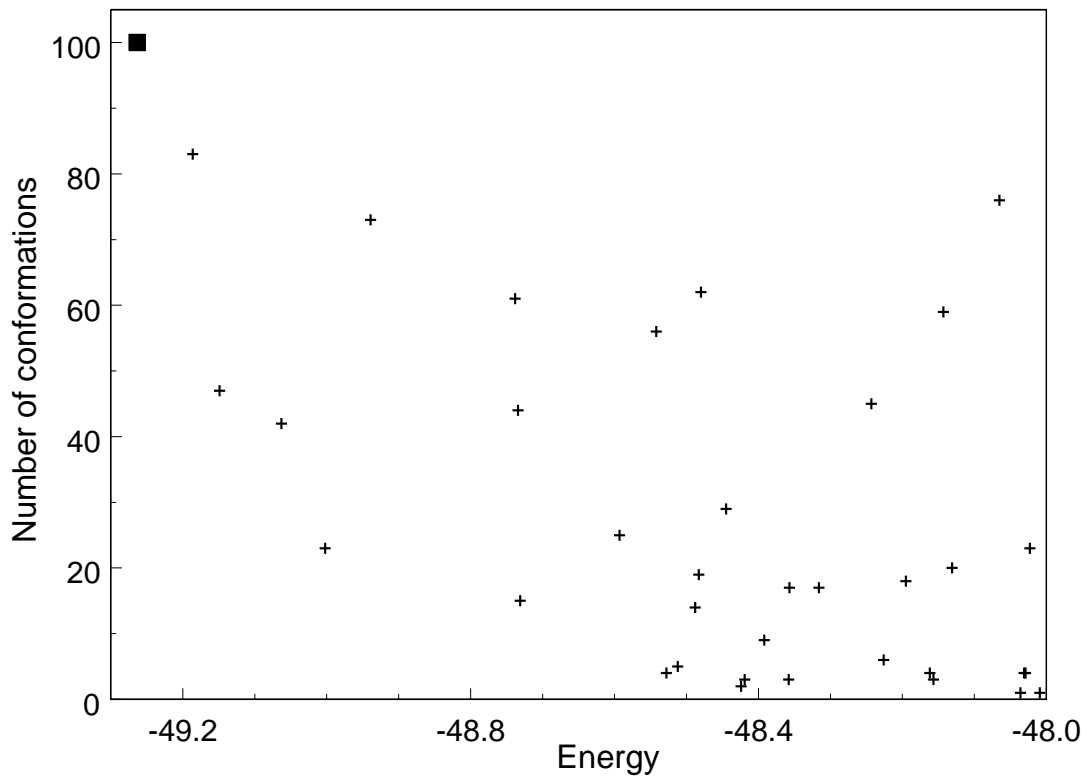


FIG. 4: The number of conformations as a function of energy for $E \leq -48$, accumulated from all 100 independent runs. The closed square represents the number of the global minimum-energy conformation with energy $E_0 = -49.2635$.

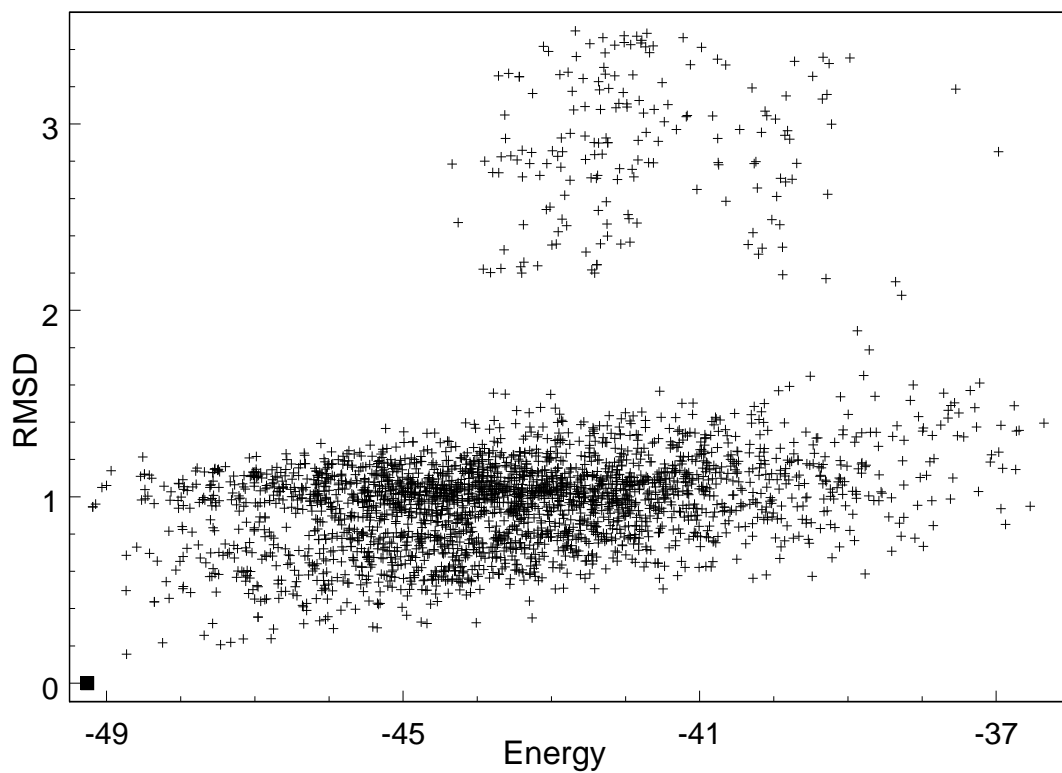


FIG. 5: Distribution of the RMSD values as a function of energy for all 2361 conformations calculated from one of the two global minima. The closed square represents the global minimum-energy conformation with energy $E_0 = -49.2635$.

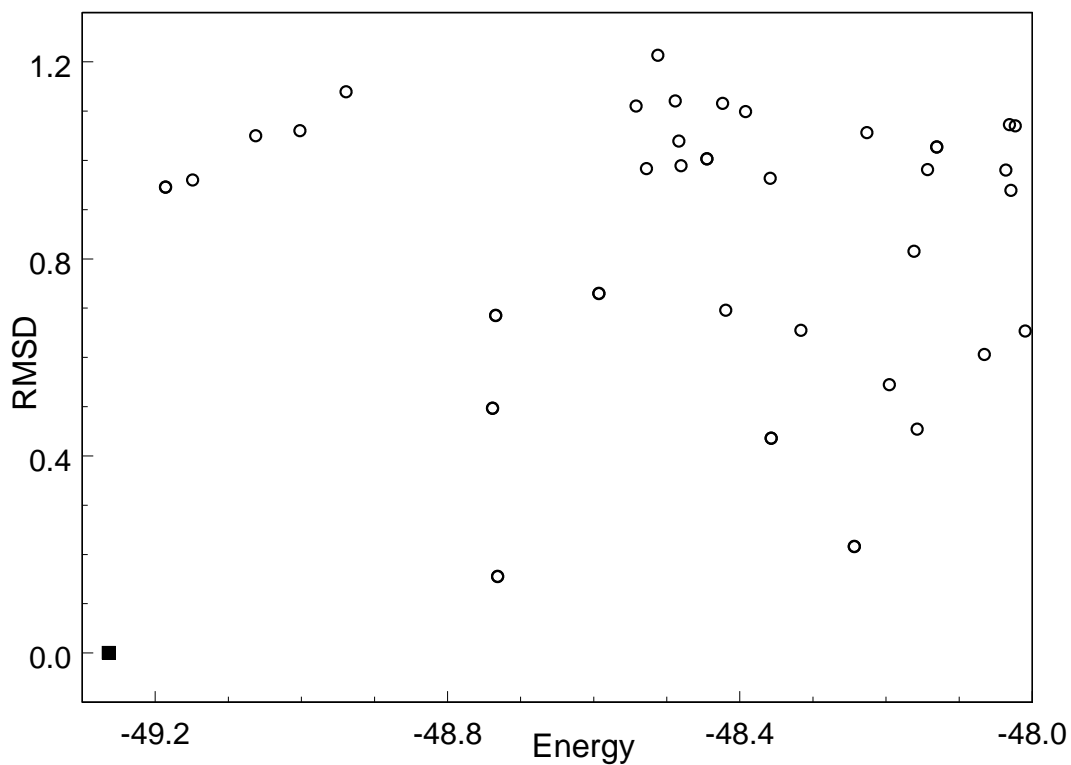


FIG. 6: Distribution of the RMSD values as a function of energy for conformations with energy $E \leq -48$ (an enlargement of the lower left corner of Figure 5). The closed square represents the global minimum-energy conformation with energy $E_0 = -49.2635$.

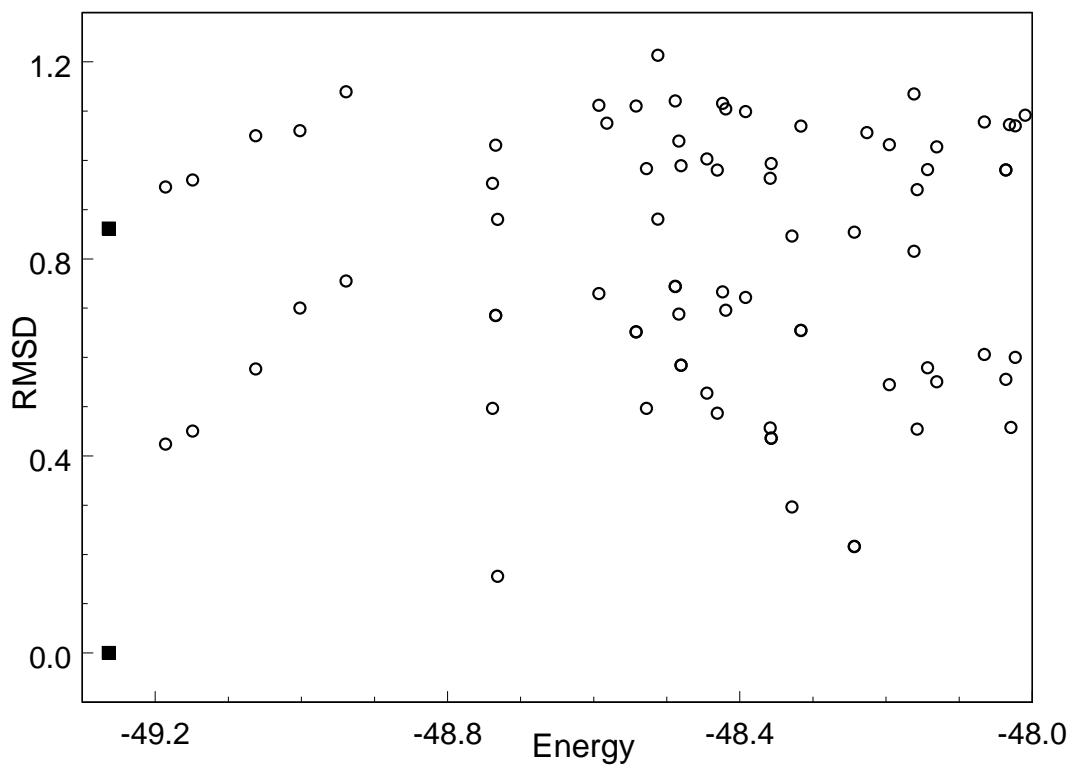


FIG. 7: Distribution of the RMSD values as a function of energy for conformations with energy $E \leq -48$, obtained from 100 CSA runs without employing the inversion symmetry. Two closed squares represent the global minimum-energy conformations with energy $E_0 = -49.2635$ connected by the inversion transformation.